



Journal of Geophysical Research: Biogeosciences

RESEARCH ARTICLE

10.1002/2015JG003035

Key Points:

- Recovery time is more sensitive to disturbance type than to intensity
- Increased carbon uptake following initial 5year recovery after disturbance
- 10-20% increase in cumulative NEE 90years past early-successional PFT mortality

Supporting Information:

- Supporting Information 51
- Data Set 51
- Data Set 52
- Data Set 53
- Software 51

Correspondence to:

R P.d.M.Frasson, frasson.l@osu.edu

Citation:

Frasson, R.P.d.M.G.Bohrer, D.Medvigy, A.M.Matheny, T.H.Morin, C.S.Vogel, C.M.Gough, K.D.Maurer, and P.S.Clrtis (2015), Modeling forest carbon cycle response to tree mortality: Effects of plant functional type and disturbance intensity, J. Geophys. Res. Biogeosci., 120, 2178-2193, doi:10.1002/2015/G003035.

Received 24 APR 2015 Accepted 1 OCT 2015 Accepted article online 11 OCT 2015 Published on line 5 NOV 2015

Modeling forest carbon cycle response to tree mortality: Effects of plant functional type and disturbance intensity

Renato Prata de Moraes Frasson¹, Gil Bohrer1, David Medvigy, Ashley M.Matheny, Timothy H.Morin, Christoph S.Vogel, Christopher M. Gough, Kyle D. Maurer1, and Peter S. Curtis

¹Department of Civil, Environmental, and Geodetic Engineering, Ohio State University, Columbus, Ohio, USA, ²Department of Geosciences, Princeton University, Princeton, New Jersey, USA, ³University of Michigan Biological Station, Pellston, Michigan, USA, ⁴Department of Biology, Virginia Commonwealth University, Richmond, Virginia, USA, ⁵Department of Evolution, Ecology, and Organismal Biology, Ohio State University, Columbus, Ohio, USA

Abstract Natural and anthropogenic disturbances influence ecological succession and impact the carbon cycle. Understanding disturbance effects and ecosystem recovery is essential to carbon modeling. We hypothesized that (1) species-specific disturbances impact the carbon cycle differently from nonspecific disturbances. In particular, disturbances that target early-successional species will lead to higher carbon uptake by the postrecovery, middle- and late-successional community and (2) disturbances that affect the midsuccessional deciduous species have more intense and long-lasting impacts on carbon uptake than disturbances of similar intensity that only affect the early-successional species. To test these hypotheses, we employed a series of simulations conducted with the Ecosystem Demography model version 2 to evaluate the sensitivity of a temperate mixed-decid uous forest to disturbance intensity and type. Our simulation scenarios included a control (undisturbed) case, a uniform disturbance case where we removed 30% of all trees regardless of their successional status, five cases where only early-successional deciduous trees were removed with increasing disturbance intensity (30%, 70%, 85%, and 100%), and four cases of midsuccessional disturbances with increasing intensity (70%, 85%, and 100%). Our results indicate that disturbances affecting the midsuccessional deciduous trees led to larger decreases in carbon uptake as well as longer recovery times when compared to disturbances that exclusively targeted the early-successional deciduous trees at comparable intensities. Moreover, disturbances affecting 30% to 100% of early-successional deciduous trees resulted in an increased carbon uptake, begin ning 6 years after the disturbance and sustained through the end of the 100year simulation.

1. Introduction

Natu ral and anthropogenic disturbances impact ecological succession, carbon dynamics, and hydrology. Forest harvesting and wildfires that occurred in the early twentieth century in the upper G reat Lakes region of North America were a primary determinant of the trajectory that led to the cu rrent composition of forest stands in northern Lower Michigan, USA [Gough et al., 2007]. Large-scale intensive logging and forest fires throughout the upper Midwest a century ago led to the establishment of many even-aged aspen-dominated forests in the region [Bergen and Dronova, 2007; Frelich and Reich, 1995]. However, as many of these stands transition from even to uneven aged with the gradual decline of early-successional aspen, less severe, non-stand replacing disturbances are playing an increasingly important ecological role as these forests advance in age [Frelich and Reich, 1995].

Each decade, up to half of the forested land in the United States is affected by disturbances including insect defoliation, disease, fire, windthrow, and selective harvest [Birdsey et al., 2006]. These disturbances vary in specificity, with some disturbances targeting individual species or genera and others acting as generalists, and also in the extent to which they cause tree morality. For example, Gypsy moth (Lymantria dispar L) defoliation affected mostly oak trees in the Silas Little Experimental Forest in New Jersey, USA [Renninger et al., 2014; Schafer et al., 2010; Schafer et al., 2014], and beech bark disease targets Fagus grandifolia (American beech) in the northeastern USA [Lovett et al., 2006]. Other disturbances such as forest ground fires and windth row are less selective. Yet specifying which species are affected and the intensity of the disturbance may not be sufficient to predict the impact of disturbance on C02 flux, as stand age and disturbance

02015.American Geophysical Union. All Rights Reserved.



history have been shown to be important factors controlling carbon cycli ng and storage [Pregitzer and Euskirchen, 2004]. In addition, forested landscapes are a mosaic of ecosystems shaped by varying levels of disturbance intensity, with the extent of tree morality potentially affecting the rate at which ecosystems recover from disturbance [Peters et al., 2013]. Understanding how disturbances varying in specificity and intensity affect forest processes central to biogeochemical cycling is integral to predicting future carbon stocks and fluxes [Knohl et al., 2002; Undroth et al., 2009; Luo and Weng, 2011].

A combination of experimental studies and model simulations provide insight i nto how and why carbon fluxes are affected by different types and intensities of forest disturbance. For example, *Clark et al.* [2010] used eddy covariance measurements of C0₂ fluxes at oak dominated sites in New Jersey, USA, to show that annual net C0₂ flux decreased by more than 40% following defoliation by Gypsy moth. In complementary work, *Medvigy et al.* [2012] showed that accurate prediction of the effects of Gypsy moths on forest carbon dynamics requires the correct identification of the spatial and temporal patterns of defoliation. In contrast to the decreased carbon uptake following the disturbances analyzed by these two studies, work at the Forest Accelerated Succession Experiment (FASET) conducted at the University of Michigan Biological Station (UMBS) has shown very strong short-term resilience to species-specific moderate-intensity disturbance [Gough et al., 2013; Matheny et al., 2014; Nave et al., 2011; Stuart-Haentjens et al., 2015].

In the present work, we aim to answer the following two questions:(1) What are the differences in the short-(years) and long-term (decades) forest carbon dynamics following species-specific and nonspecific disturbances of similar mag nitudes? and (2) How does disturbance intensity, or extent of tree mortality, affect ecosystem recovery time and postrecovery net ecosystem exchange? We leverage observations from the Forest Accelerated Succession Experi ment (FASET)-a large-scale ecological manipulation where all early-successional trees in a 34 ha plot were killed by stem gird ling, which provides the means to evaluate our carbon flux predictions d uring and following our simulated disturbances. We used the Ecosystem Demog raphy model version 2 (ED2) [Medvigy et al., 2009] to simulate the impact of moderate disturbance on carbon fluxes from a temperate mixed-deciduous forest. We produced a set of simulations differing in disturbance intensity and specificity to assess their impact on recovery time and postdisturbance carbon dynamics. We compared the control simulation results with observed site-level net ecosystem exchange at the unaltered AmeriFl ux-affiliated US-UMB site in northern Lower Michigan, USA (http://ameriflux.oml.gov/fu llsiteinfo.php?sid=S9), whereas we evaluate our predictions of carbon flux d uring and after the simulated disturbances against data collected by the US-UMd tower, which is nested within the FASET disturbance.

2. Materials and Methods

2.1. Ecosystem Demograph y Model 2

ED2 resolves energy, water, carbon, and nitrogen balances on representative individuals, belonging to biologically similar vegetation groups (defined here as Plant Functional Types, PFTs) [Medvigy et al., 2009; Medvigy et al., 2013; Moorcroft et al., 2001]. The individuals within each PFT are further grouped into age/size cohorts. While the PFT defines the cohorts physiological parameters, which do not change with plant height or age, the size class controls the cohorts access to resources. Cohorts belonging to the same resource environment ("patch" in the model's internal termi nology) compete for light, nutrients, and water. The model tracks the growth, reproduction, and mortality by changing the stem density of each cohort. As the trees within a cohort grow, they move to the next size class. Reproduction increases stem density of the smaller size classes, and mortality reduces the stem density of the corresponding cohort.

Cohort-level gross primary production, net primary production, and heterotrophic respiration are calculated using parameterizations for radiative transfer, leaf biophysics, photosynthesis, and respiration [Medvigy et al., 2012;Medvigy et al., 2009;Medvigy et al., 2013]. Cohort-level predictions of, for example, net ecosystem $\rm CO_2$ exchange (NEE) and latent and sensible heat fluxes are scaled to the patch level through the cohorts stem density. Fi nally, patch-level predictions are scaled to the site-level by area-weighted integral averaging over all resource environmental patches.

In order to evaluate the long-term (decades to a century) impact of disturbance scenarios on NEE, it was necessary to create a disturbance algorithm that allowed for the decomposition of dead biomass affected by the disturbance. The disturbance routine we developed allows the specification of one or more mortality



events. During such events, mortality, which is specified as a fraction of the stem density of each cohort of a specified PFT, occurs and the selected trees die instantly. The dead biomass is immediately returned to the soil, including its nitrogen content. The returned biomass is free to decompose, providing a more realistic representation of element cycling relevant to postdisturbance heterotrophic respiration and long-term net ecosystem exchange. Although mortality prescribed under our disturbance routine occurs instantaneously, specification of successive small events can emulate gradual mortality. To simulate the gradual death of a fraction, f, of the trees of a given PFT each month during over f years, the monthly mortality rate is given by

$$m1 = \frac{f}{-1} \frac{1-1}{1} \frac{1}{-1} - \frac{1}{12-nj=1-mi}$$
 (1)

where m_1 is the fraction of current number of trees of the PFT that the user intents to remove at month iand m_4 stands for the imposed mortality at a previous month j.

After mortality events, affected patches may be split if disturbed area is greater than the minimum area allowed for a patch. The vegetation contained in the original patch is redistributed between the newly created patches. One will receive the undisturbed fraction of the vegetation, retaining the premortality stem density of the original patch, whereas the second will receive the remaining surviving trees, resulting on a sparser patch. Next, ED2 searches all patches for cohorts with negligible stem density, which are eliminated, or for similar cohorts, which are combined. Two cohorts can be combined if they are of the same PFT and if their mean DBH is within the model's preset tolerance. ED2 source code can be found in the supporting information {Software SI}.

2.1.1. Meteorological Drivers

We forced ED2 with observations from the control plot adjacent to the FASET experimental site {available through the AmeriFlux network, site id US-UMB). The FASET field site, located at the University of Michigan Biological Station in northern Michigan, consists of two plots-the experimental plot {Ameri Flux site id US-UMd, 45°33'45"N, 84°4154"W) and the control plot {US-UMB, 45°33'35"N 84°4249"W). Approximately 35% of the basal area of the forest in the site is dominated by early-successional, relatively even aged *Populus grand-identata* Michx.{bigtooth aspen), *Populus tremuloides* Michx.{trembling aspen), and *Betula papyrifera* Marsh. {paper birch). Other species that comprise significant fractions of the canopy include *Fagus grandifolia* Ehrh. {American beech), *Acer saccharum* Marsh.{sugar maple), *Acer rubrum* L {red maple), *Pinus strobus* L.{white pine} and *Quercus rubra* {red oak). The early-successional aspen and birch species are currently beginning to senesce and will continue to do so over the next 50 years [Curtis *et al.*, 2005; *Gough et al.*, 2010,2013]. In spring 2008,all ear1y-successional aspen and birch trees in a 34 ha plot were stem girdled, totaling approximately 64-00 trees. For a detailed description of the experiment and an empirical analysis of the FASET disturbance effects and subsequent ecosystem recovery, refer to *Gough et al.* [2013]. The control plot remained undisturbed. Each plot is located within the footprint of an eddy-covariance flux tower.

The observations we used to drive ED2 include air temperature (T_0), wind direction and speed, atmospheric surface-level pressure, relative humidity {rH}, surface CO_2 concentration, photosynthetically active radiation {PAR} separated into direct-beam and diffuse fractions, and downward long and short wave radiation. Short-term gaps in the data were filled by fitting a linear relationship between the measurements made at US-UMB and the nearby measurements at US-UMd. We used 5 years of meteorological forcing (2007-2011), which we recycled during the 6 years that preceded 2007 and the 89 past 2011. Partitioning between beam and diffuse short-wave radiation was assumed identical to the partitioning of PAR into its beam and diffuse fractions. The meteorological forcing can be found in Data Set SI in the supporting information.

2.1.2. Model Initialization and Configuration

We initialized our simulations using tree species and diameter at breast height {DBH} recorded in 60 permanent plots of approximately 0.1 ha within the US-UMB flux footprint in 2001 {included in the supporting information Data Set S2}. Tree diameters were measured repeatedly over time allowing the calculation of individual tree growth rates and mortality {deaths per number of surveyed trees per year) $[Gough\ et\ al,\ 2013]$. According to the 2001 census, basal area {BA} per ground area of all surveyed trees totaled 24.6 m² ha-², while in 2010, it reached 26.4 m² ha-²-. Table 1 shows the groupings of the different species according to PFT and their contribution to the total BA.

The mineral fraction of the soil surrounding the US-UMB and US-UMd flux towers contains 920*b* sand, 7% siltand 1% clay [Curtis *et al.*, 2005; *Nave et al.*, 2009], which ED2 uses to derive soil characteristics, eg., permeability. Soil depth and carbon content were derived from *Nave et al.* [2011], and nitrogen content from *Nave et al.* [2013].

Table 1. Distribution of Species and Plant Functional Types According to Fraction of the Total Basal Area According to the Censuses of 2001 and 2010 Conducted at UMBSa

		Fraction of the Total BA	
Plant Functional Type	Species	2001	2010
Early-successional hardwood	Populus grandidentata Michx.	0.38	0.37
	Populus tremu/oides Michx.	0.13	0.12
	Betu/a papyrifera Marsh.	0.09	0.07
Midsuccessional hardwood	Quercus rubra L.	0.10	0.12
	Acerrubrum L	0.16	0.18
Late-successional hardwood	Fogus grandifo/ia Ehrh.	0.03	0.04
	Acer saccharum Marsh.	0.01	0.01
Northern pine	Pinus strobus L.	0.08	0.09
aThe total basal area per ground	l area in 2001 was 24.6 m ² ha- ² while in 20	10, it reached the value	of $26.4 \mathrm{m}^2 \mathrm{ha}^{-2}$.

Initial soil temperature was assumed to be uniform at all depths and equal to the air temperature at initialization, after which it was allowed to drift according to the model's estimation of heat flux throughout soil layers. Initial soil moisture was assumed to be 0.18 m³/m³ as measured at the US-UMB site on 01 January 2001.

We chose to prescribe phenology using the observed seasonal dynamics of leaf area index {LAI) in order to improve the realism of the simulations. We used measurements of LAI conducted in the UMBS from 1999 to 2011 using LAI-2000 Plant Canopy Analyzers {Li-Cor, Lincoln, NE, USA) to create a time series of LAI throughout the growing season {for a summary of the LAI seasonal dynamics, refer to *Curtis et al.* [2005] and *Garrity et al.* [2011]). We normalized the LAI by the peak LAI in the season and fitted a double sigmoidal curve to the normalized LAI {supporting information Data Set S3). Using this fitted curve, we produced a time series of daily fraction of total LAI, which ED2 used to control the growth and senescence of leaves in the deciduous PFTs.

2.1.3. Model Optimization

A preliminary single-site, 6 year simulation using the northeastern North American parameterization of ED2 [$Medvigy\ et\ al.$, 2009] showed an unrealistic and sharp decline of the basal area of all PFTs. This unexpected behavior prompted us to search for parameter values estimated in areas dominated by early- and middle-successional vegetation growing on predominantly sandy soils, as is the case of the UMBS forest. We therefore adopted the values of the photosynthetic capacity per unit leaf area ($V_{\rm cmax}$ as in $Farquhar\ et\ al.$ [1980]), growth respiration fraction { $r_{\rm o}$ }, and water availability parameter { $K_{\rm w}$ } from $Medvigy\ et\ al.$ [2012].

Additionally, we decreased the specific leaf area {SLA} of the early-successional deciduous PFT from its default value of $30\,\mathrm{m}^2\,\mathrm{kg}^{-1}$ to $255\,\mathrm{m}^2\,\mathrm{kg}^{-1}$ and the SLA of the late-successional deciduous PFT from the default value of $60\,\mathrm{m}^2\,\mathrm{kg}^{-1}$ to $30.6\,\mathrm{m}^2\mathrm{kg}^{-1}$ to reflect site values reported by $Gaugh\ et\ al.$ [2010]. Finally, we used a fine root turnover rate of $0.56\mathrm{yr}^{-1}$ for the middle- and late-successional PFTs from $Gill\ and\ Jackson$ [2000], based on measurements by $Hendrick\ and\ Pregitzer$ [1993] for a forest located in northern lower Michigan.

We followed the approach used by M edvigy et al. [2013] for model optimization. Our optimization included eight parameters: (1) a multiplier for the Vcmax of the deciduous early-, middle-, and late-successional PFTs {i.e.,one single value that multiplied the Vcmax of early-, middle-, and late-successional deciduous PFT, avoiding their individual optimization), (2) the conifer $Vcma^{"}$ (3) the allocation of fine roots relative to leaves for the deciduous PFTs {same value for the three PFTs), (4) growth respiration factor { r_{0} } for the deciduous PFTs, (5) the stomata! response slope (M, assumed the same for the three deciduous PFTs), (6) the rainfall interception capacity,(7) the water availability parameter {Kw}, and (8) the fraction of positive carbon balance devoted to reproduction {same value for the three deciduous PFTs}.

We assumed independent gamma distributions as the prior distribution of each one of eight parameters. We used the method of moments to find the shape and the scale parameters of each gamma distribution so that the expected value of each prior matched the values listed in Table 2, and we assumed the standard deviation of each prior to be 10 times the standard deviations of the posterior distributions reported by $Medvigy\ et\ al.\ [2009]$. The exception was the $Vext{cmax}$ multiplier for which we assigned an expected value of 1 and standard deviation of 08.

Table 2. List of Parameters Used in our Simulations That Differ From ED2's Standard Parameterizationa

Parameter Value

Parameter Name	Unit	Symbol	hitial	Optimized
Photosynthetic capacity per unit leaf area, conifer Photosynthetic capacity per unit leaf area, early hardwood Photosynthetic capacity per unit leaf area, midhardwood Photosynthetic capacity per unit leaf area, late hardwood Allocation of fine roots relative to leaves, hardwoods	μ molm- 2 s- 2 (kgroots)(kg leaves)- 1	Vcmax Vcmax Vcmax Vcmax	11.4 20.4 17.5 7.0 1.1	9.6 26.5 22.7 9.1
Growth respiration factor, hardwood Stomata! slope hterception capacity Water availabity parameter, hardwood Fraction of positive carbon balance devoted to reproduction	dimensionless dimensionless kgm- ² m2 yr - ¹ (kg root)- ¹ dimensionless	fg M inter Kw repro	0.12 4 0.33 2500 029	0.17 3.68 0.46 2700 0.53

aVcmax hereis specified at 15°C.

Each iteration of the Markov chain Monte Carlo consisted of a 3year simulation (2007, 2008, and 2009). As censuses of the UMBS vegetation were conducted in 2001 and repeated in 2010, we chose the 2010 data set, which is the closest to the beginning of the optimization runs (2007). We forced ED2 with half-hourly measu rements of meteorological forcing from US-UMB in 2007 to 2009. The observed and model-predicted values of monthly and yearly total N EE, nightti me respiration, and gapped latent and sensible heat fluxes computed for the years of 2008 and 2009 (2007 was discarded for model spin-up) were used to evaluate the log-likelihood at each iteration:

$$S = \sum_{j=1}^{N_{\text{datasets}}} \left(\frac{W_j}{N_j} \cdot \sum_{i=1}^{N_j} (s_{ij}) \right)$$
 (2)

where N_1 is the number riobservations in the data set j (24 for monthly variables and 2 for yearly variables), is the weight rithe data set j, and s/J is the contribution of the element if rom the data set j to the log-likelihood function, which, assuming a normal distribution for the measurements errors for the data set j, has the form of

$$Sij = -\frac{1}{2} \cdot \frac{(Xpred.ij - Xobsjj)^{2}}{Clij}$$
 (3)

where $x_{pred}y$ is the value of the variable j as predicted by ED2 at the given iteration, $x_{obs}y$ is the observed value for the variable, and c_{TIJ} is the standard deviation of the error associated with the data set. Details on the flux data processing including the estimation of the error standard deviation are included in the Appendix A.

Because we utilized gapped monthly and yearly measurements of latent heat and sensi ble heat fluxes in the computation of the log-likeli hood, we disregarded model predictions duri ng these gaps. For this procedure, we first aggregated ED2's prediction into half-hou rly bins, which were considered in the computation of the yearly and monthly totals on ly if correspondi ng measurements were present. This proced ure was not necessary when computing the monthly and yearly NEE totals, as we gap-filled NEE.NEE uncertainty was evaluated by combining measurement errors evaluated according to *Richardson and Hollinger* [2005] with gap-fill uncertainty as detailed in the Appendix A.

We used the calculated log-likelihood to evaluate the acceptance probability of the current realization:

$$a = \min(1, \text{lft-s}_{-}, -i)). \tag{4}$$

where sk is the log-likelihood function evaluated at iteration k, sk-1 is the log-likelihood function evaluated at iteration k-1, and sk' is the sum of the log-likelihoods associated with each parameter.

We ran 10separate chains with 10000 iterations each. At the end of the proced ure, we obtained a pool of 883 accepted iterations, from which, after burn-in, we computed the posterior distribution of each parameter. The parameter set that corresponded to the highest likelihood was selected for use in the simulations.

2.1.4. Model Evaluation

We ran two simulations to evaluate the control run's predictions and a third to eval uate our disturbance simulations. The first run utilized preoptimization parameters {Table2, initial parameters} to provide a benchmark

Table 3. List of Simulation Scenariosa

Simulation Scenario	Parameter Set	Disturbance Type
Preliminary run	initial set	none
Undisturbed	optimized set	none
UNIF	optimized set	30% removal of PFTs
G100	optimized set	gradual removal of 100% early successional deciduous PFT
E30	optimized set	30% removal of early-successional deciduous PFT
E70	optimized set	70% removal of early-successional deciduous PFT
E85	optimized set	85% removal of early-successional deciduous PFT
E100	optimized set	100% removal of early-successional deciduous PFT
M70	optimized set	70% removal of midsuccessional deciduous PFT
M85	optimized set	85% removal of midsuccessional deciduous PFT
M100	optimized set	100% removal of midsuccessional deciduous PFT

aWith the exception of the preliminary run, which ran from 1January 2008 to 31 December 2013, all other scenarios ran from 1January 2001 to 31 December 2101.

for the evaluation of model optimization. The second and the third runs employed the optimized set of parameters as listed in Table 2.We initialized all three simulations using the 2001 census data. For the third run, we emulated the gradual mortality of the FASET experimental disturbance by spreading the mortality of the early-successional deciduous trees across 2years {GI00}. On the first day of each month, beginning on 1 January 2008 and ending 1 January 2010, the disturbance routine killed a fraction of the trees belonging to the early-successional PFT. This resulted in 24 events with mortality rates calculated by equation (1), where f=l,n=2.

We compared the two {preoptimization and optimized) control cases' monthly and yearly predictions of NEE to the observations collected during 2007, 2010, 2011, 2012, 2013, and 2014 at the US-UMB control site. Since we constrained the model using fluxes observed in 2008 and 2009, we excluded these years from the computation of the model-fit statistics. We evaluated the two control simulations' predictions based on coefficient of determination {r2} between monthly measurements and predictions of NEE and the 6 year total NEE. We used monthly rather than half-hourly aggregation for evaluation to avoid the effects of trivial correlations due to strong diurnal cycles.

Measured and predicted monthly NEE used in the computation of r2 only included fluxes that occurred when instruments were functional and when the measured friction velocity exceeded 0.35 ms- 1 [Gough et al., 2013; Maurer, 2013]. We evaluated biases in our model by comparing yearly NEE and the accumulated NEE from 2007 to 2014 with gap-filled observations collected at the US-UMB tower. Since computation of yearly carbon fluxes included gap-filled observations, we estimated yearly carbon flux uncertainties by combining measurement and gap-filling uncertainties as detailed in the Appendix A. Additionally, we compared the predicted NEE with observed yearly totals computed using two different gap-fill techniques: the marginal distribution sampling {MDS} [Reichstein et al., 2005] and the Max Planck Institute for Biogeochemistry's eddy covariance gap-filling and flux-partitioning tool {http://www.bgc-jena.mpg.de/-MDlwork/eddyprocl}. We evaluated our third simulation, the FASET-like disturbance {GI 00}, against site-level net ecosystem exchange observed by the US-UMd disturbance tower from 2009 to 2014.

2.2. Simulation Scenarios of Disturbance Type and Severity

We ran 10scenarios (Table 3): a control (undisturbed) case and 9 disturbance cases where we tested the influence of the intensity and type {PFT specificity or which PFT was affected) of disturbance on carbon cycling pools and fluxes. The 10 runs began on 01 January 2001, to allow for model spin-up before the prescription of the disturbances, and ran for 100 years. This simulation length allows for 90 years after the prescription of the simulations, which is approximately the time that it took for the forest in northern Lower Michigan to develop to its current state since the large-scale disturbances that affected the area.

In the control case, we prescribed the initial conditions directly from the census observations of 2001 and did not prescribe disturbances throughout the course of the simulation. In the uniform disturbance case {UNIF}, we killed 30% of individuals of each size class, regardless of PFT, on the first day of 2010. We ran four disturbance cases where only early-successional deciduous trees were killed on the first day of 2010, with varying

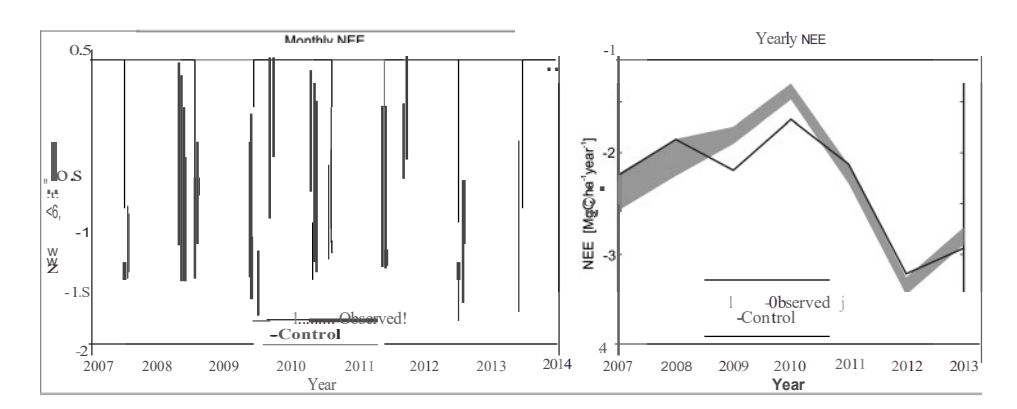


Figure 1.Optimized ED2 monthly NEE predictions (after calibration) during the model evaluation period. On the left panel, the dotted line represents the monthly NEE measured at the US-UMB site, while the solid line represents ED2's predictions. On the right panel, the solid line shows ED2's predictions of yearly NEE, while the shaded area represents the observed yearly NEE with a 1-standard deviation uncertainty envelope. For a detailed explanation on the computation of C02 flux uncertainty computations, refer to Appendix A.

intensities: 30% {E30), 70% {E70), 85% {E85), and 100% {E100). We ran three disturbance cases where 70%, 85%, and 100% of midsuccessional deciduous trees were killed {M70, M85, and MIOO, respectively).

We tested an additional disturbance scenario emulating the mortality rate in the FASET experiment, where we prescribed the mortality of all early-successional deciduous trees gradually, from January 2008 to January 2010 (GI 00). Unlike the other abrupt disturbance scenarios, the mortality imposed under the GIOO case was gradual, to better mimic the elongated period of mortality observed after stem girdling at the FASET site. The GI 00 disturbance consisted of 24 monthly events, with mortality rates calculated with equation (1). Each event occurred on the first day of each month, from January 2008 to January 2010.

3. Results and Discussion

3.1. Model Evaluation

Initial parameter corrections to the late-successional SLA, middle- and late-successional fine root turnover rate, $Verna'''r_g$, and Kw for the conifers and middle- and early-successional deciduous PFTs {Section 2.1.3} led to an improvement in r^2 from 0.77 to 092 between model predictions and observations of monthly NEE and prevented the unrealistic mortality observed in the preliminary run. After optimization, monthly r^2 remained equal to 092. However, the optimization reduced the differences between the observed and predicted accumulated 6 year carbon flux from -30% {preoptimized run} to 806 {optimized run}. Postoptimization differences were mostly driven by larger {less negative} than observed NEE during the summers of 2007 and 2011 and larger {more positive} than observed NEE during the winter of 2009 {Figure I, left panel}.

The largest differences between ED2s predictions and the observed carbon flux at the US-UMB tower happened in 2009 and 2010 {Figure 1}. The overestimation of NEE during the year of 2010 could be connected to a forest tent caterpillar (Malacosoma disstria) infestation that happened that year and affected both the control and FASET plots which would have likely decreased the observed carbon uptake [Gough et al., 2013]. However, as it was beyond the scope of this experiment, we did not include the 2010's infestation in our simulations.

As we computed yearly carbon fluxes utilizing gap-filled data, we tested two additional gap-fill techniques to evaluate the impact of the chosen method on the model-data agreement. During the period of 2007-2014 {excluding the optimization years of 2008 and 2009}, the total NEE gap-filled using the artificial neural network {ANN} method {see Appendix A} amounted to approximately -14.1MgC ha-¹ When gap-filled following the MOS method, the corresponding carbon flux was approximately -16.9 MgC ha-¹ Use of the Max Planck institute for Biogeochemistry's Eddy covariance gap-filling and flux-partitioning tool resulted in carbon flux of -116 MgC ha-¹ This quick comparison illustrates how the choice of gap-filling technique can impact the computation of yearly carbon fluxes, as discussed in detail by Wang et al. [2015]. Differences were not so pronounced when we tested the three gap-fill techniques on the US-UMdsite, where

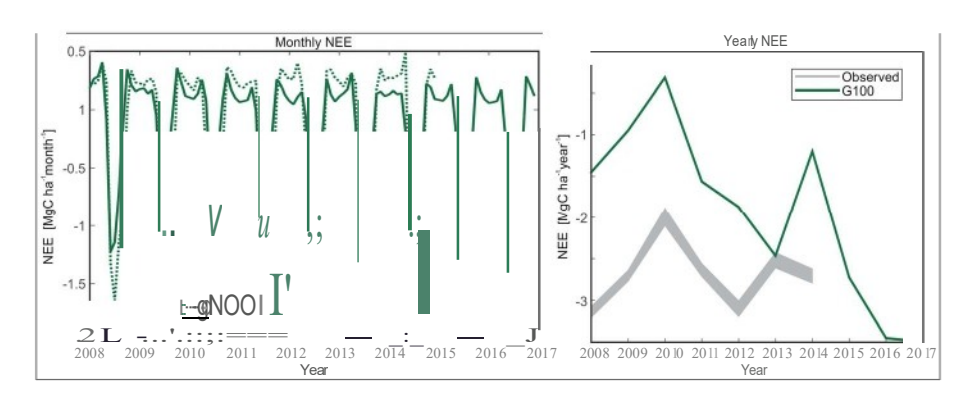


Figure 2. Left panel: time series of the modeled, monthly, plot-level NEE for the G100 disturbance (gradual 100% removal of early-successional trees) from 2007 to 2017. The solid green line shows modeled NEE, while the dotted black line shows 5 years of observations recorded at the US-UMd tower, which underwent a similar prescribed disturbance in 2008. Right panel: solid line represents ED2's predictions of yearly NEE, while the shaded area represents the observed yearly NEE at the US-UMd tower with a 1-standard deviation uncertainty envelope.

the ANN, MOS, and the eddy covariance gap-filling and flux-partitioning tool approaches led to an accumulated carbon flux of -188 MgC ha⁻¹ -180 MgC ha⁻¹ and -21.0 MgC ha⁻¹ respectively, for 2008-2014.

Comparing our gradual disturbance case (Gl 00), under which trees of the early-successional decid uous PFT were killed from January 2008 to January 2010, with observed fluxes from the US-UMd tower (overlooking the FASET experiment), we found that simulations overestimated the impact of this disturbance on carbon uptake (Figure 2). Our simu lation showed a decrease in carbon uptake following the Gl 00 disturbance comparable to what previous observational studies reported following disturbances of comparable intensity, e.g., the review article published by Amiro et al. [2010J summarizi ng several disturbances caused by fire, harvest, insect infestation, and hurricanes, the analysis of gypsy moth defoliation in New Jersey, USA published by Clark et al. [2010] and Schiifer et al. [2010] in which oaks suffered complete defoliation, as well as in the summary of several insect and pathogen disturbances affecting 1806 to 95% of the studied canopies throughout the United States and Canada presented by Hicke et al. [2012J. Additionally, some studies showed carbon uptake decreases strong enough to cause the stand to become a carbon source, e.g., the analysis of spruce budworm (Choristoneura fumiferana Clem.) infestation of stands dominated by spruce (Picea sp.) and balsam fir (Abies balsamea L.) in eastern Canada presented by Dymond et al. [2010J, insect defoliation and forest fires located in central Canada published by Fleming et al. [2002J, and the study of pi ne beetle (Dendrodonus ponderosae Hopkins) infestations throug hout Canada presented by Kurz et al. [2008], with intensities ranging from a few affected trees in some stands up to complete mortality in other stands. Instead, fluxes at our site displayed unexpected resilience following intermediate disturbance intensity [Gough et al., 2010, 2013J, which ED2 could not reproduce.

Our simulations overestimated the impact of the disturbance and the length of ecosystem recovery during the first 4 years following the end of the imposed mortality. The simulated NEE began to show some recovery in 2013 (2years after the end of mortality), when the predictions under the Gl OO case approached the observed fluxes. The agreement between the simulation and observations was poor again in 2014, when the summer was considerably more productive in reality than in our simulations (Figure 2). However, in 2015, carbon uptake increased and the NEE was again under -2.7 Mg C ha-1 yr-1, which is comparable to the fluxes in 2013 and 2014 (-2.5 and -2.7 Mg C ha-1 yr-1, respectively). The predicted NEE remained consistently below the yearly flux of -2.7 Mg C ha-1 yr-1 observed in 2014 until 2024 (behavior similar to the El 00 curve in Figu re 4), suggesting the end of the predicted postdisturbance period of low ecosystem productivity.

A delay in modeled recovery could be partially explained by the mechanism through which the simulated forest recovered. The survivi ng middle- and late-successional trees at the FASET plot responded to the 2008's gird ling event by first increasing the photosynthetic rates of leaves from undisturbed trees and then by growing more leaves on undisturbed trees in subsequent years, replacing the lost early-successional leaf area by 2011 [Gough et al., 2013]. However, the simulated recovery following the GlOO disturbance occurred mostly by growing newly established middle- and late-successional trees.



Another explanation for the overestimation of the recovery time by our simulation could be related to an underestimation of the postdisturbance light-use efficiency {LUE). *Gough et al.* [2013J found that during partial defoliation of the stem-girdled trees {peaking in 2010}, increased LUE and rapid replacement of leaf area by the unaffected trees were responsible for the sustained carbon uptake observed at the treatment site following the disturbance. Indeed, the treatment sites canopy apparent quantum yield was higher than the control site's following disturbance during all years except 2010, suggesting that rapid canopy physiological shifts compensated for a temporary reduction in leaf area from disturbance.

In our simulations, the removal of LAI, particularly that of the taller cohorts, increased light penetration in the canopy. However, increased illumination of previously shaded cohorts in our simulations was insufficient to reproduce the observed increase in LUE. This indicates that following the disturbance, the remaining vegetation could have a larger light-driven physiological capacity,or in ED2s terminology, the leaf-level quantum efficiency. Experimental work conducted by *Gough et al.* [2013J and *Cheng et al.* [2015J show that physiological traits controlling the LUEcould vary over time as the vegetation recovers from a disturbance. However, the model assumes that parameter values are fixed properties of the PFT.As a result, ED2 does not represent an essential mechanism supporting NEE resilience at the FASET site. Nevertheless, using estimates of apparent quantum yield of the canopy from the literature [eg., *Gough et al.*, 2013J, to estimate the leaf-level quantum efficiency of each PFT presents is challenging. For example, deeper light penetration into the canopy following disturbance also increases the rate of leaf carbon fixation of formerly shaded vegetation and is difficult to distinguish from enhanced leaf physiological competency since both phenomena have similar effects on canopy LUE [Niinemets, 2010J.

The adoption of time dependent $V_{cma}X!$ with higher photosynthetic capacity immediately after a disturbance, decreasing asymptotically to the original value of V_{cmax} could increase the recovery speed and provide a mean to better describe the observed results. Alternatively, one could assume that V_{cmax} and quantum efficiency of the leaves change with tree height, as sun and shade leaves have different responses to increased light exposures. Both directions present their own challenges, as the parameterization of dynamic V_{cmax} would require measurements of carbon flux following disturbances of different intensities and affecting different PFTs. The latter approach would require measurements of quantum efficiency and V_{cmax} to be made at different canopy levels and the scaling of the measured parameters from leaf-level to canopy level, which is often not trivial.

3.2. Postdisturbance Recovery

In the control case, the model showed a continuous decline of the early-successional PFT aboveground biomass (AGB), which was slowly replaced by the growing midsuccessional PFT AGB (Figure 3a). The gradual replacement of early-successional by midsuccessional trees predicted by our simulations is consistent with the behavior observed in the 2001 and 2010 censuses (Table 1) and previously reported for our site [Gough et al., 2010J. According to the predicted distribution of AGB, the early- and middle-successional species will compose a similar portion of the total AGB by 2023 and the late-successional AGB will remainstable.

The gradual death of the early-successional deciduous trees observed at the UMBS forest {decrease in basal area shown under Table 1) and simulated in the control scenario {see Figure 3a) reallocated growth-limiting resources to the midsuccessional deciduous PFT $[Gough\ et\ al.,\ 2013;Matheny\ et\ al.,\ 2014;Nave\ et\ al.,\ 2011J.$ Upon accessing the newly available resources, the simulated midsuccessional PFT responded with a sharp increase in AGB from 2011 to 2022 {Figure 3a). This period of simulated increases in AGB corresponds with observed increases in CO $_2$ uptake from 2011 to 2013 {Figure 1). Eventually, the simulated increased productivity tapers off for two reasons: (1) increased heterotrophic respiration caused by the decomposition of the dead organic matter and (2) the stagnation of the midsuccessional growth.

In the uniform disturbance case {Figure 3b), we found a similar decreasing trend in early-successional AGB that persisted after the disturbance. The midsuccessional PFT grew rapidly after the disturbance event, recovering 80% of the lost AGB over the course of 12 years. The E70 and E85 cases showed similar behaviors {E85 case shown in Figure 3e). In both E70 and E85, the midsuccessional PFT showed rapid aboveground biomass growth for the 10 years following the disturbance. After this period, the growth of the midsuccessional PFT slows to a rate similar to that of the control case.

The EI00 {instantaneous mortality of all early-successional deciduous trees pictured in Figure 3f) and GI00 {gradual mortality of early-successional deciduous trees over 2years) showed similar results and differed only

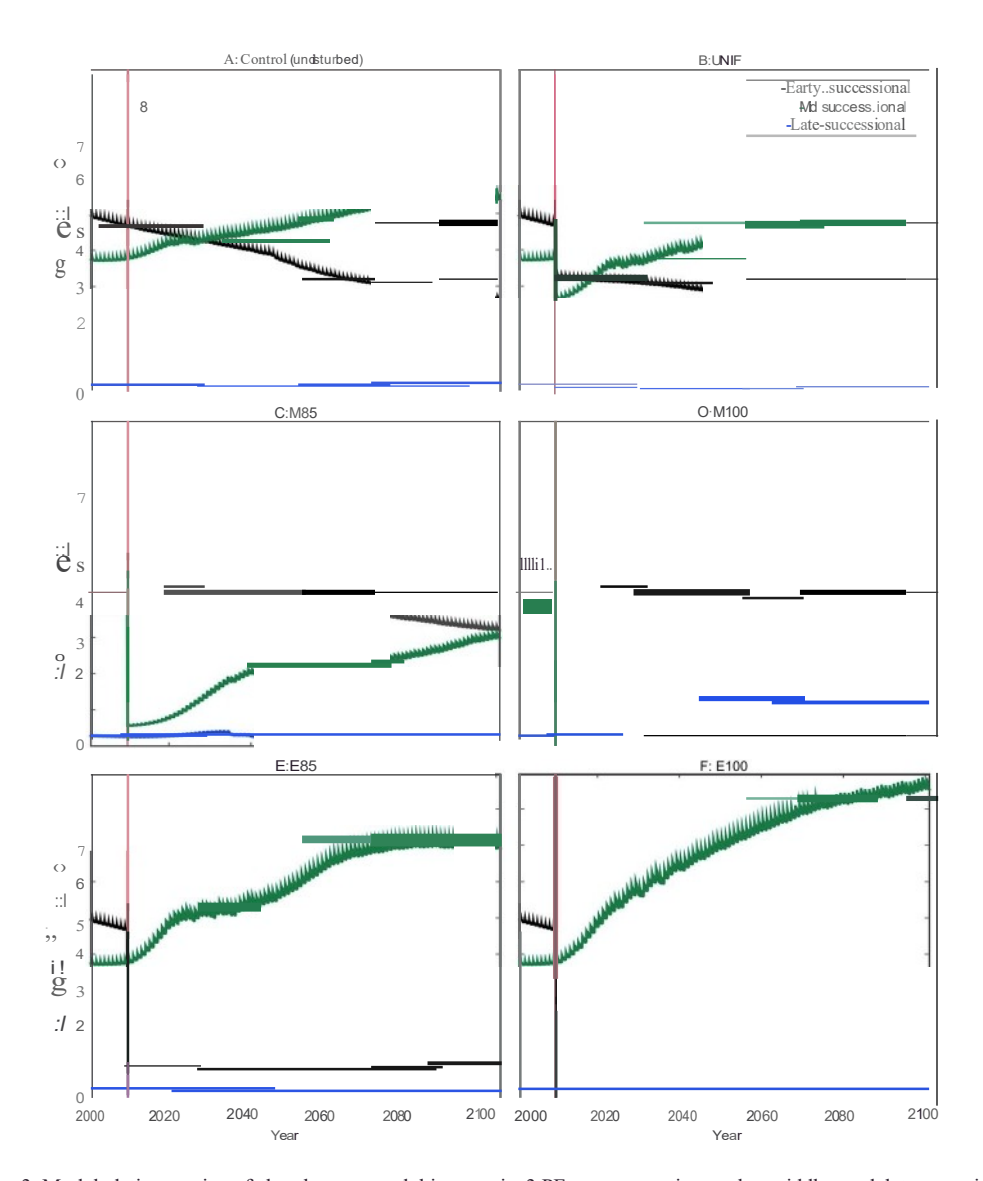


Figure 3. Modeled time series of the aboveground biomass in 3 PFrs, representing early-, middle-, and lateuccessional deciduous trees in UMBS during the first century of simulations: (a) Control case. (b) Uniform disturbance case (UNIF). The sudden drop in the AGB of the three PFrs represents the disturbance event, when 30% of all trees were killed. (c) Disturbance case (M85), where 85% of the midsuccessional trees were killed. (d) M100 case where all midsuccessional trees were killed. (e) Case E85, where 85% of all early-successional trees were killed. (f) Complete removal *c:i* early-succession al trees (case E100). The vertical red line present in all panels designates the year of the disturbance.

during a short period immediately following the initial prescription of the disturbance. When compared to EIOO, the gradual GIOO case showed increased loss of NEE but faster recovery in the S years following the disturbance, and was closer to the gradual mortality of trees in FASET and the observed response of NEE [Gough et al., 2013]. During the first 14 postdisturbance years, midsuccessional AGB sustained greatest growth in the GIOO and EIOO scenarios relative to other simulated disturbance scenarios {Figure 3f}. Unlike the milder early-successional disturbances {E30, E70,and E85), after the end of GIOO and EIOO events, there were no early-successional trees left,which prevented further recruitment of early-successional trees. For this reason, there was no recovery of the lost early-successional AGB {Figure 3f}.

Increasing disturbance intensities among the E-type (from 30% to 100%) disturbances was associated with more rapid growth ri the midsuccessional AGB (Figures 3e and 3f). Within our simulations, the mortality imposed by the disturbance event resulted in increased resource availability to the surviving cohorts, which may explain their increased postdisturbance growth rate. More intense disturbances result in higher resource availability among

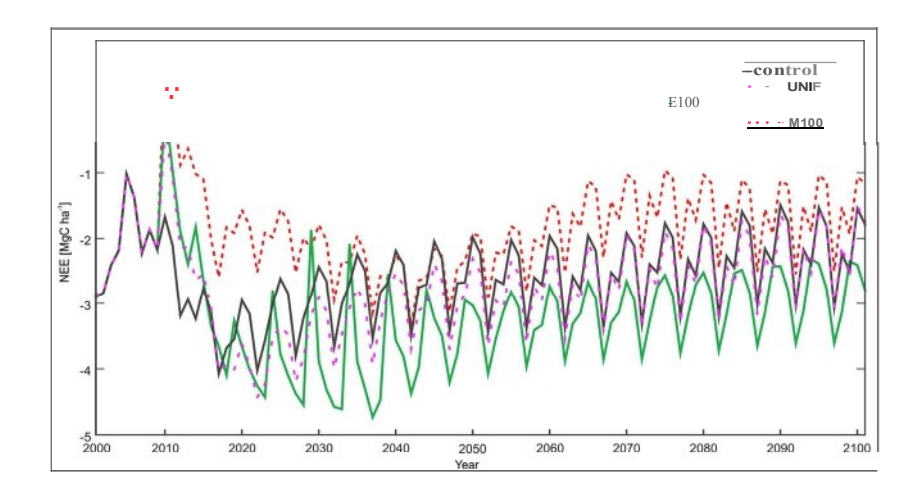


Figure 4. nme series of modeled, monthly, plot-level NEE in the full 100 years *ci* simulations, for cases of no disturbance (control, solid black line), uniform disturbance (UNIF, dotted magenta line), EIOO disturbance, (100% removal of early-successional deciduous PFT, solid green line), and MI00 (100% removal of midsuccessional deciduous PFr, dotted red line). The 5 year cycles in NEE visible in this figure are a result of recycling 5 years of meteorological forcing throughout the simulation.

the remaining trees both by reallocation of nutrients contained in the dead trees and by diminished competition, as the disturbance decreases the number of trees competing for light water, carbon, and nitrogen.

Figures 3c and 3d show the impact of hypothetical disturbances affecting midsuccessional cohorts only. In the scenario M85 (85% removal of midsuccessional deciduous trees, shown in Figure 3c), the remaining midsuccessional trees show increased growth following the 2010's disturbance. However, this growth is slower than observed under the E85 and El00 cases and AGB lost to the M85 event is not fully recovered by the end of the simulation. Under the MIOO case (100% removal of midsuccessional deciduous trees, pictured Figure 3d), the removal of the midsuccessional trees reduces the mortality rate of the early-successional deciduous cohorts and is followed by a growth of late-successional AGB. However, the growth of the late-successional deciduous AGB is not enough to fully compensate for the loss in midsuccessional biomass.

Simulations targeting different successional cohorts, early or middle, suggest that the recovery time of NEE depends on the PFT affected by disturbance. Under the UNIF and E30, E70, E85, and El00 disturbance simulation-scenarios and in our FASET observations, the initial disturbance period was followed by recovery with higher C0₂ uptake {more negative NEE) than the predisturbance baseline {El00, Ml00,and UNIF shown under Figure 4). However, disturbances exclusively affecting the midsuccessional PFT (70%,85%,and 100% mortality rates under cases M70, M85, and Ml00, respectively) never experienced higher C0₂ uptake than the control scenario {Ml00 shown under Figure 4). The annual NEE under the E70, E85, El00, and UNIF scenarios reached the same level as annual NEE predicted by the control simulation in 2015. However, the EIOO and UNIF disturbances of equivalent intensity {both scenarios affected 30% of the stand's LAI) differed in their impact on postrecovery carbon fluxes. While UNIF carbon uptake began to decrease after 2023, EIOO sustained the elevated carbon uptake rates until past 2035. Interestingly but not surprisingly, since UNIF did not change the forest relative composition, NEE under the UNIF disturbance converged to similar levels as the control simulation and after 2062 became indistinguishable from the control scenario.

The lack of recovery observed of the M-type disturbances {disturbances affecting 70% to 100% of the midsuccessional deciduous PFT) could be related to the current successional dynamics taking place in northern Michigan [Gough et al., 2010J. In the E-type disturbances {disturbances exclusively affecting early-successional deciduous PFTs), we removed only early-successional deciduous trees, which were already in decline at this site, consequently freeing resources to longer-lived growing midsuccessional deciduous trees. After an initial period of less intense carbon uptake following the E-type disturbances, which lasted from 4 {E30, E70, and E85} to 5years {EOO}, the disturbed simulations showed stronger carbon uptake. Whereas in the M-type cases, the prescribed disturbance affected the growing midsuccessional deciduous trees, which are the primary successional cohort supporting forest growth as early-successional trees decline [Gough et al., 2010J. Consequently, the period of increased carbon uptake was attenuated {M70} or did not occur {M85 and MI00} following mortality of middle-successional trees.

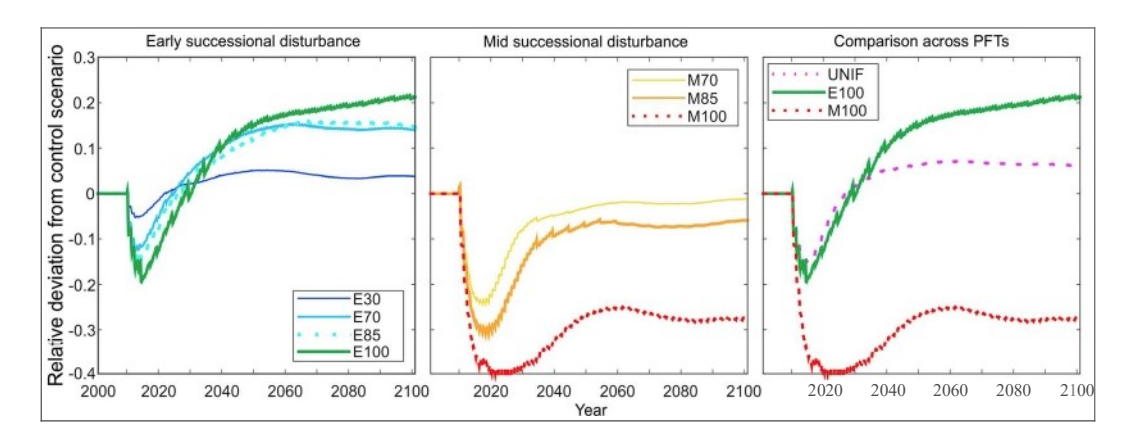


Figure 5. The effect of different levels of disturbance on the accumulated net ecosystem exchange. This effect was measured as the relative deviation from the accumulated NEE in the control case, therefore, dimensionless. Negative values represent times when the accumulated NEE since the beginning of the simulation for a particular scenario was less than the accumulated NEE at the control case. The left panel compares four different intensities of disturbances affecting the early-5uccessional deciduous PFT. The middle panel compares three different disturbance intensities affecting the midsuccessional PFT only. The panel on the right compares the uniform distribution (UNIF) with ElOO and MIOO disturbances. The 5 year cycles visible in this figure are a result of recycling 5 years of meteorological forcing throughout the simulation.

The lengthoftime needed for the accumulated NEE from a particular scenario to equal the accumulated NEE in the control (undisturbed) scenario represents an integrative metric of ecosystem recovery. By analyzing accumulated NEE since disturbance instead of individual years, we can assess whether longer-term increases in carbon uptake following the E-type and UNIF disturbances can compensate for reduced carbon uptake immediately after disturbance.

Focusing on the E-type disturbances {Figure 5, left panel), increasing disturbance intensity led to more pronounced decreases incarbon uptake inthe first 3 {E30} or 5years {E100}. Under the E30 case, the cumulative difference inNEE between disturbed and control scenarios was lowest in 2013 {-5%}, after which the yearly NEE of E30 surpassed that of the control. The short-term (0 to 5 years) cumulative reduction in NEE increased with disturbance intensity, declining relative to the controls in 2013 by -12.7% and -156% in E70 and E85 scenarios, respectively; however, the E100 disturbance scenario did not reach a minimum until2015, amounting to a reduction of -19.5% relative to the control scenario, indicating that the effects of the most intense disturbance were stronger and lasted longer.

Among E-type disturbances, the time required to surpass the accumulated NEE of the simulated control forest increased with disturbance intensity. For example, the accumulated NEE under the E30 case first surpassed the accumulated control NEE in 2022, whereas this event happened for E70 in 2025, in 2026 for E85 2026, and 2029 under the E100 case. Additionally, increasing mortality of already declining early-successional species led to increased long-term (30 to 100years) carbon uptake. E100 and G100 both showed greater accumulated carbon uptake of approximately 20% relative to the control at the end of the 100 year simulation, while E70 and E85 showed increases of 14% and 15%, respectively {Figure 5, right pane0. Such long-term increases in carbon uptake following disturbance are consistent with simulation results reported by *Albani et al.* [2010J, who predicted an initial decrease in carbon uptake after a simulated hemlock woolly adelgid (*Adelges tsugae Annand*) infestation, followed by an average postrecovery increase in carbon uptake of 12% throughout the eastern United States.However, ecosystems subjected to repeated disturbance events of high intensity,eg, recurrent insect defoliation events, may not have the chance to recover from each event [Medvigy et al., 2012] and consequently not show the predicted long-term increase carbon uptake.

The initial negative impact on carbon uptake of disturbances affecting the midsuccessional deciduous PFT was similar to early-successional disturbances. Higher disturbance intensities caused larger initial decreases in carbon uptake {Figure 5, middle panel) and minimum NEE to occur later (2017 under M70, 2019 under M85, and 2025 under MI00). However, the behavior of the middle- and early-successional disturbances became quite different following the trough in NEE. Twenty-five to 30years after the occurrence of early-successional and UNIF disturbances, the ecosystem carbon uptake surpassed that of the control



scenario. Nevertheless, we never observed such increase in ecosystem production when we disturbed the midsuccessional vegetation.

Greater long-term {decades after the disturbance} carbon uptake following the mortality of early- {E-type} rather than middle- {M-type} successional trees may be associated with the first disturbance targeting short-lived trees past peak growth and the second targeting longer-lived vigorously growing trees [Nave et al., 2011]. Increasing cumulative productivity with increasing mortality of early-successional trees indicates that, at the current ecological successional stage, communities of midsuccessional trees are more productive while declining early-successional trees contribute proportionally less to ecosystem production. This is supported by the smaller increase in long-term carbon uptake {6%} seen under the UNIF case, which removed a smaller percentage of the less productive early-successional trees and also removed an equal fraction of midsuccessional trees, as well as by the decrease in both short- {few years to a decade} and long-term {decades to a century} carbon uptake under disturbances that affected the midsuccessional deciduous PFT. Despite the lack of an experimental study comparable to FASET that assesses the effects of the removal of midsuccessional deciduous trees, our simulations, along with observations from the FASET site [Gough et al., 2013; Stuart-Haentjens et al., 2015], suggest that disturbances that hasten ecological succession can have positive impacts on long-term carbon budgets and reinforce the importance of correctly prescribing which PFTs are affected by simulated disturbances.

4. Conclusion

Our ED2 simulations demonstrated that under nonstand-replacing disturbances of moderate i ntensity, the impacts on postdisturbance NEE and recovery time were substantially different depending on the successional status of the affected trees and the level of disturbance intensity. While the mortality of 30% to 100% of the early-successional deciduous trees led to a decrease in carbon uptake immediately after the disturbance, it was followed by increased carbon uptake in the following decades. The same behavior was not observed under the simulated midsuccessional mortality, nor under the nonspecific disturbance. The mortality of 70% to 100% of the midsuccessional deciduous trees led to a decrease in carbon uptake both immediately as well as decades after the disturbance, with increasing mortality associated with a more pronounced decrease in carbon uptake. Moreover, the NEE under the tested nonspecific disturbance slowly recovered and became indistinguishable from the control 52 years after the treatment. Our findings stress the importance of correctly specifying the successional status of trees affected by a modeled disturbance. Additionally, our results suggest that ecosystems may recover more quickly from disturbances that selectively affect tree populations or communities al ready in decline, by reallocating resources to vigorously growing trees.

Appendix A: Flux Data Processing and Uncertainty Analysis

The optimization procedu re requi red knowledge of the monthly and yearly net ecosystem exchange {NEE}) and sensible (HJ and latent {Le}) heat fluxes as well as an assessment of their u ncertainty. We used the 2010 fluxes measu red at the US-UMB tower for model optimization. We employed the US-UMB data from the years of 2007, 2008, 2009, 2011, 2012, 2013, and 2014 for model evaluation.

We processed the data following AmeriFlux convention. The detailed data processing is described in *Maurer* [2013] and *Gough et al.* [2013]. Data were filtered using a friction velocity, u^* , threshold following *Reichstein et al.* [2005]. Specific seasonal threshold values used for our site are listed in *Maurer et al.* [2013]. We separated the year in three seasons: dormant, early growth, and late growth. During the dormant season, we attributed all carbon flux to respiration $\{f^*\}$? (i.e., no photosynthesis). During the early- and late-growth seasons, all nighttime carbon flux was due to Re^* . As large gaps were present in the Re data series $\{both\ because\ no\ growing\ season\ daytime\ observations\ were possible and the fact that the <math>u^*$ filter tends to eliminate several adjacent flux values), we gap-filled Re by modeling through the use of equation $\{A1\}$, which was evaluated for our site by $Schmid\ et\ al.\ [2003]$:

$$Re = a \cdot exp(b \cdot Tsoil) + c \cdot SM + d \cdot ln(SM)$$
 (A1)

where a, b, c, and d were empirically fitted constants, T_{50} n stands for the soil temperature at 20 mm, and SM for the soil moisture. Equation $\{A1\}$ was also used to model Re at known half hours for error calculation purposes. The difference between the observed and modeled Re was used to estimate the gap-filling error.



We subtracted the modeled daytime Re from the observed carbon flux to determine the observed gross primary prod uctivity {GPP}. We used the artificial neural network {ANN} method to gap-fill GPP as described in *Morin et al.* [2014a], which is an expanded version of the approach developed by *Papale and Valentini* [2003]. The ANN method creates empirical models with user defined predictor variables as the parameters. We used air temperature (T) relative humidity {rH}, total PAR, diffuse PAR, *Albedo, SM*, T_{5011} and wind velocity as the predictor variables. These variables are not dependent on turbulence and were measured by robust sensors with only sparse data gaps.

We were therefore able to gap-fill the predictor variables prior to use in the ANN by using a linear periodic method, which is suitable for short, sporadic gaps. The ANN first normalized all variables between 0 and 1. It then took the predictor variables, assigned them random weights to each, and passed them through a hyperbolic tangent sigmoid {tansig} transfer function to produce a 'hidden-layer' of 12 nodes. This layer was passed through a second tansig transfer function to generate a hidden-layer with five nodes. This was then passed th rough a final tansig transfer function to produce the output layer.

The AN N used a random 50% of the data to parameterize the training set, another nonoverlapping 25% to validate the parameter estimates, and the remaining 25% to the test the model {i.e., calculate r). The minimum permissi ble r2 set for the ANN model was 0.8. If the output layer was able to meet or exceed this value, we took the output layer as one modeled realization of GPP. If not, the process was repeated until a suitable model realization was found. The parameterization of the ANN models is done with a random number generator and is allowed to converge to the observed values. Because of this, there are endless possible models it may generate to replicate a given data stream. For our purposes, no one model is more valid than any other, and to mitigate the possibility of an erroneous model, we generated 1000independent model realizations for GPP and took the average of these realizations as the final modeled value. Specific information regarding the ANN setup and approach can be found in Morin et al. [2014a] and Morin et al. [2014b].

We quantified the measurement uncertainty for GPP using the approach described by *Hollinger and Richardson* [2005], which considers the differences between observations that were separated by 24 h as an indication of random measurement error, provided that the environmental conditions under which they were taken were similar. The criteria to establish the similarity of measurement conditions were as follows: PAR measurements did not differ by more than 75µmol m-2 s-1 the air temperature was within 3"C, and the average wind speeds measured at both times were not more than 1 ms-1 apart. To each half-hour with valid measurements we added noise, which we consider to have a double-exponential distribution with zero mean and the scaling parameter estimated from the variance of the measurement error estimates [Richardson et al., 2006].

We used the spread of all 1000 realizations of the AN N to characterize the variability of the gap-filled GPP data points. For each gap-filled half-hour, we picked one of the 1000 possible estimates for that half-hour, which came from the different realizations of the AN N. We computed the monthly and yearly totals then repeated the procedure 1000 times. At the end of the procedure, we obtained 1000 estimates for each month's fluxes and 1000 estimates for the yearly flux.

Following the completion of the *Richardson and Hollinger* [2007] proced ure, we used a Monte Carlo simu lation to combine the uncertainty due to measurement errors and the uncertainty from the gap-filling procedure. We averaged all estimates for each month as the observed flux for that month and the standard deviation of the monthly estimates as the uncertainty for that specific month. Similarly, we calculated the yearly flux as the average of the yearly flux estimates, while the uncertainty was represented by the standard deviation of the yearly flux estimates. Since latent and sensible heat fluxes were not gap-filled, their uncertainty only reflects measurement errors.

For the eval uation of possible measurement biases introduced by the gap-fill method, we tested two additional gap-filling methods, i.e., the marginal distribution sampling {MDS} by *Reichstein et al.* [2005] and the Max Planck Institute for Biogeochemistry's eddy covariance gap-filling and flux-partitioning tool {http://www.bgc-jena.mpg.de /-MDlwork/eddyprocl}. The MDS method consists of replacing missing NEE values by the average NEE observed under similar meteorological conditions and contained in a time-window of \pm 7 days from the missi ng value. Meteorological similarity was defined as two half-hours when the average net radiation, air temperature, and vapor pressure deficit did not deviate by more than 50Wm-², 25"C, and 5.0hPa, respectively. The second additional gap-filling method is based on *Falge et al.* [2001] with the



addition of the temporal autocorrelation of fluxes and the conditioning of fluxes by meteorological variables as described in *Reich5tein et al.* [2005].

The eddy covariance gap-filling and flux-partitioning tool [MaxPlanck Institute for Biogeochemistry, 2011] classifies gaps into three groups. In the first group, NEE is missing {either due to instrument failure or insufficient turbulent mixing), but all meteorological data are available. In this situation, meteorological similitude can be tested using the same conditions as identified by $Reich5tein\ et\ al.\ [2005]$. In the second group, in addition to a missing NEE value, meteorological variables {air temperature or vapor pressure deficit) are missing as well, but radiation is available. In this case, meteorological similitude is based solely on solar radiation. Under the third situation, radiation is also missing. In the first and second scenarios, the algorithm searches for half-hours with similar meteorological conditions contained within a 7 day window. If no NEE data are available inside this window, the search is expanded first to 14 days then 28 or 56 days as needed, with the wider windows flagged as less reliable. Under the third condition, the missing value is obtained by linear interpolation between available adjacent information with an initial time window of 0.5 days, which can be extended to up to 2.5 days in the absence of data.

Acknowledgments

The study was funded by the National Science Foundation, Hydrological Science project 1521238, the U.S. Department of Energy's Office of Science, Office of Biological and Environmental Research, Terrestrial Ecosystem Sciences program under awards DE-SC0006708 and DESC0007041, and the AmeriFlux Management project under Flux Core Site agreement 7096915 through Lawrence Berkeley National Laboratory. Model simulations ran at the Ohio Supercomputer Center under allocation award PAS0409-4 and at the Great Lakes Consortium for Petascale Computation under a BlueWaters project award. Eddy covariance data utilized to drive and evaluate the simulations is freely available through the AmeriFlux portal (http://ameriflux. lbl.gov/). We would like to thank the four anonymous reviewers for their constructive criticism of our manuscript

References

- Albani, M., P. R Moorcroft, A M. Ellison, D. A. Orwig, and D.R. Foster (2010), Predicting the impact of hemlock woolly adelgid on carbon dynamics of eastern United States forests, Can. J. For. Res., 40, 119-133, doi:10.1139/x09-167.
- Amiro, B. D., et al. (2010), Ecosystem carbon dioxide fluxes after disturbance in forests of North America, J. Geophys. Res., 115, GOOK02, doi: 10.1029/2010/JGOO1 390.
- Bergen, K. Mand I.Dronova (2007), Observing succession on aspen-dominated landscapes using a remote sensing-ecosystem approach, Landscape Ecol., 22, 1395-1410, doi:10.1007/s10980-007-9119-1.
- Birdsey, R., K. Pregitzer, and A. Lucier (2006), Forest carbon management in the United States: 1600-2100, J. Environ. Qual., 35, 1461-1469, doi:10.2134/jeq20050162.
- Cheng, S.J., G. Bohrer, A. L. Steiner, D. Y. Hollinger, A. Suyker, R. P. Phillips, and K. J. Nad elhoffer (2015), Variations in the influence of diffuse light on gross primary productivity in temperate ecosystems, *Agric. For. Meteorol.*, 201,98-110, doi:10.1016/j. agrformet.2014.11002.
- Clark, K. L, N. Skowronski, and J. Hom (2010), Invasive insects impact forest carbon dynamics, *Global Chantje Biol.*, 1688-101, doi:10.1111/j. 1365-2486.2009.01983.x.
- Curtis, P. S., C. S. Vogel, C. M. Gough, H.P. Schmid, H.B. Su, and B.D. Bovard (2005), Respiratory carbon losses and the carbon-use efficiency of a northern hardwood forest, 1999-2003, *New Phytol.*, 167,437-455, doi:10.1111/j.1469-81372005.01438.x.
- Dym ond, C. C., E.T. Neilson, G. Stinson, K. Porter, D. A. Maclean, D. R. Gray, M. Campagna, and W. A. Kurz (2010), Future spruce budworm outbreak May create a carbon source in eastern Canadian forests, *Ecosystems*, 13917-931, doi:10.1007/s10021-010-9364z.
- Falge, Eet al. (2001), Gap filling strategies for long term energy flux data sets, Agric. Far. Meteorol., 107, 71-77.
- Farquhar, G.D., S. V. Caemmerer, and J. A. Berry (1980), A biochemical model ci photosynthetic C0₂ assimilation in leaves of C₃ species, *Planta*, 14978-90, doi:10.1007/bf00386231.
- Fleming, R. AJ. N. Candau, and R. S. McAlpine (2002), Landscape-scale analysis of interactions between insect defoliation and forest fire in Central Canada, *Qim. Change*, 55, 251-272, doi:10.1023/a:1020299422491.
- Frelich, L. E., and P. B. Reich (1995), Spatial patterns and succession in a Minnesota southern-boreal forest, Ecol. Manogr., 65, 325-346, doi:10.2307/2937063.
- Garrity, S. R, G. Bohrer, K. D. Maurer, K. L. Mueller, C. S. Vogel, and P. S. Curtis (2011), A comparison of multiple phenology data so1Xces for estimating seasonal transitions in deciduous forest carbon exchange, Agric. Far. Meteorol, 151, 1741-1752, doi:10.1016/j. agrformet2011.07008.
- Gill, R. A., and R. B. Jackson (2000), Global patterns of root turnover for terrestrial ecosystems, New Phyto/., 147, 13-31, doi:10.1046/j. 1469-81372000.00681.x.
- Gough, C. M., C. S. Vogel, K. H. Harrold, K. George, and P. S. Curtis (2007), The legacy of harvest and fire on ecosystem carbon storage in a north temperate forest, *Global Chantije Bia/*, 13 1935-1949, doi:10.1111/j.1365-2486.200701406.x.
- Gough, C. M., C. S. Vogel, B. Hard iman, and P. S. Curtis (2010), Wood net primary production resilience in an unmanaged forest transitioning from early to middle succession, Far. Ecol. Manage., 260, 36-41, doi:10.1016/j.foreco.2010.03027.
- Gough, C. M.,B. S. Hardiman, L. E. Nave, G. Bohrer, K. D. Maurer, C. S. Vogel, K. J. Nadelhoffer, and P. S. Curtis (2013), Sustained carbon uptake and storage following moderate dist1Xbance in a Great Lakes forest, *Ecol. Appl.*, 23, 1202-1215 doil 0.1890/12-1554.1.
- Hendrick, R. L, and K. S. Pregitzer (1993), The dynamics of fine-root length, biomass, and nitrogen-content in 2 northern hardwood ecosystems, Can *J. Far. Res.*, 23,2507-2520, doi:10.1139/x93-312.
- Hicke, J. A, et al. (2012), Effects of biotic disturbances on forest carbon cycling in the United States and Canada, Global Change Biol., 1B, 7-34, doi: 10.1111/j. 1365-2486.201102543.x.
- Hollinger, D. Yand A. D. Richardson (2005), Uncertainty in eddy covariance measurements and its application to physiological models, *Tree Physiol.*, 25, 873-885, doi:10.1093/treephys/257873.
- Knohl, A., 0. Kolle, T.Y. Minayeva, I.M. Milyukova, N. N. Vygodskaya, T. Foken, and E. D. Schulze (2002), Carbon dioxide exchange of a Russian boreal forest after disturbance by wind throw, *Global Change Biol.*, 8,231-246, doi: 0.1046/j.1365-2486.2002.00475.x.
- Kurz. W. A,C. C. Dymond, G. Stinson, G.J. Rampley, E.T. Neilson, A. L. Carroll, T. Ebata, and L. Safranyik (2008), Mountain pine beetle and forest carbon feedback to climate change, *Nature*, 452, 987-990, doi:10.1038/nature06777.
- $Lindroth, A., F.\ Lagergren, A.\ Grelle, L.\ Klemedtsson, 0. Langvall, P.\ Weslien, and\ J.\ Tuulik (2009), Storms\ can\ cause\ ElXope-wide\ reduction\ in forest\ carbon\ sink,\ \textit{Global\ Change\ Biol.,}\ 15,346-355, doi:10.1111/j.\ 1365-2486.2008.01719.x.$
- Lovett, G. M.C. D. Canham, M.A. Arthur, K. C. Weathers, and R. D. Fitzhugh (2006), Forest ecosystem responses to exotic pests and pathogens in eastern North America, *BioScience*, 56, 395--405, doi:10.1641/0006-3568(2006)056[0395:fertep]2.0.co;2.



- Luo, Y. Q., and E. S. Weng (2011), Dynamic disequilibrium of the terrestrial carbon cycle under global change, Trends Ecol. Evol., 26,96-104, doi: 10.1016/j.tree.2010.11003.
- Matheny, A. M., et al. (2014), Species-specific transpiration responses to intermed iate disturbance in a northern hardwood forest, *J. Geophys. Res. Biogeosci*, 1192292-2311, doi:10.1002/2014JG002804.
- Maurer, K. D. (2013), Effects of Climate, Forest St111cture, Soil Water, & Scale an Biosphere-atmosphere Gas Exchange in a Great Lakes Mixed-deciduaus Forest, 203 pp., The Ohio State Un iv., Columbus, Ohio.
- Maurer, K. D., B. S. Hardiman, C. S. Vogel, and G. Bohrer (2013), Canopy-structure effects on surface roughness para meters: Observations in a Great Lakes mixed-deciduous forest, *Agric. Far. Metearol.*, 177, 24-34, doi:10.1016/j.agrformet.201304.002.
- Max Planck Institute for Biogeochemistry (2011), Eddy covariance gap-filling and flux-partitioning tool Retrieved September 24, 2015, from [Available at http://www.bgc-jena.mpg.de/-MDlwork/eddyproc/methodphpJ
- Medvigy, D., S. C. Wofsy, J. W. Munger, D. Y. Hollinger, and P.R. Moorcroft (2009), Mechanistic scaling of ecosystem function and dynamics in space and time: Ecosystem Demography model version 2, J. Geophys. Res., 114, GO1002, doi:10.1029/2008JG000812.
- Medvigy, D.K. L. Clark, N. S. Skowronski, and K. V. R Schafer (2012), Simulated impacts of insect defoliation on forest carbon dynamics, Environ. Res. Lett, 7,045703, doi:10.1088/1748-9326/7/4/045703.
- Medvigy, D., S.J. Jeong, K. L. Clark, N. S. Skowronski, and K. V. R. Schafer (2013), Effects of seasonal variation of photosynthetic capacity on the carbon fluxes of a tern perate deciduous forest, J. Geophys. Res. Biogeasci, 11B, 1703-1714, doi:10.1002/2013/G002421.
- Morin, T.H.G. Bohrer, L. Naor-Azrieli, S. Mesi, W. T.Kenny, W. J. Mitsch, and K. V. R. Schafer (2014a), The seasonal and diurnal dynamics of methane flux at a created urban wetland, *Ecol. Eng.*, 72,74-83, doi:10.1016/j.ecoleng201402.002.
- Morin, T.H.G. Bohrer, R. P. d.M. Frasson, L. Naor-Azreli, S. Mesi, K. C. Stefanik, and K. V. R. Schafer (2014b), Environmental drivers of methane fluxes from an urban temperate wetland park, J. Geophys. Res. Biogeosci, 119, 2188-2208, doi:10.1002/2014JG002750.
- Moorcroft, P.R., G.C. Hurtt, and S.W. Pacala (2001), A method for scaling vegetation dynamics: The ecosystem demography model (ED), Ecol. Managr., 77(4), 557-585.
- Nave, L. E., C. S. Vogel, C. M. Gough, and P. S. Curtis (2009), Contribution of atmospheric nitrogen deposition to net primary productivity in a northern hardwood forest, *Can. J. Far. Res.*, 39, 1108-1118, doi:10.1139/x09-038.
- Nave, L. E, et al. (2011), Disturbance and the resilience ci coupled carbon and nitrogen cycling in a north temperate forest, J. Geophys. Res., 116 G040 16, doi:10.1029/2011JG00 1758.
- Nave, L.E.K. J. Nadelhoffer, J. M. Le Moine, L.T.A van Diepen, J. K. Cooch, and N.J. Van Dyke (2013), Nitrogen uptake by trees and mycorrhizal fungi in a successional northern temperate forest: Insights from multiple isotopic methods, *Ecosystems*, 76(4), 590-603, doi: 10.1007/sl 0021-012-9632-1.
- Niinemets, U. (2010), A review of light interception in plant stands from leaf to canopy in different plant functional types and in species with varying shadetolerance, *Ecol. Res.*, 25, 693-714, doi:10.1007/s11284-010-0712-4.
- Papale, Dand A. Valentini (2003), A new assessment of European forests carbon exchanges by eddy fluxes and artificial neural network spatialization, Global Change Biol., 9, 525-535, doi:10.1046/j.1365-2486.200300609.x.
- Peters, E. B., K. R. Wythers, J.B. Bradford, and P. B. Reich (2013), Influence of disturbance on temperate forest productivity, *Ecosystems*, 16, 95-110, doi:10.1007/s10021-012-9599-y.
- Pregitzer, K. S., and E. S. Euskirchen (2004), Carbon cycling and storage in world forests: Biome patterns related to forest age, *Global Change Biol.*, 102052-2077, doi:10.1111/j.1365-2486200400866.x.
- Reichstein, M., et al. (2005), On the separation *ci* net ecosystem exchange into assimilation and ecosystem respiration: Review and improved algorithm, *Global Change Biol.*, 11, 1424-1439, doi:10.1111/j.1365-2486.2005.001002.x.
- Renninger, H.J.N. Carlo, K. L. Clark, and K. V. R. Schafer (2014), Modeling respiration from snags and coarse woody debris before and after an invasive gypsy moth disturbance, *J. Geophys. Res. Biogeasci.*, 119, 63 O4, doi:10.1002/2013/G002542.
- Richardson, A. D., and D. Y. Hollinger (2005), Statistical modeling of ecosystem respiration using eddy covariance data: Maximum likelih ood parameter estimation, and Monte Carlo simulation of model and parameter uncertainty, applied to three simple models, *Agric. For. Metearol.*, 131, 191-208, doi:10.1016/j.agrforrnet200505008.
- Richardson, A. Dand D. Y.Hollinger (2007), A method to estimate the additional uncertainty in gap-filled NEE resulting from long gaps in the C0₂ flux record, *Agric. Far. Metearal.*, 147, 199-208, doi:10.1016/j.agrformet.200706.004.
- Richardson, A. D.etal. (2006), A multi-site analysis of random error in tower-based measurements of carbon and energy fluxes, *Agric. For. Metearol.*, 136 1-18 doi:10.1016/j.agrfarmet2006.01007.
- Schafer, K. V. R, K. L. Clark, N. Skowronski, and E. P. Hamerlyn ck (2010), Impact of insect defoliation on forest carbon balance as assessed with a canopy assimilation model, *Global Change Biol.*, 16546-560, doi:10.1111/j. 1365-2486200902037.x.
- Schafer, K. V. R, H.J. Renninger, K. L. Clark, and D. Medvigy (2014), Hydrological responses to defoliation and drought of an upland oak/pine forest, *Hydro/. Process.*, 28,6113-6123, doi:10.1002/hyp.10104.
- Schmid, H.P.H.B. Su, C. S. Vogel, and P. S. Curtis (2003), Ecosystem-atmosphere exchange of carbon dioxide over a mixed hardwood forest in northern lower Michigan, J. Geaphys. Res., 708(D14), 4417, doi:10.1029/2002JD003011.
- Stuart-Haentjens, E,P. S. Curtis, R. T. Fahey, C. S. Vogel, and C. M. Gough (2015), Net primary production of a temperate deciduous forest exhibits a threshold response to increasing disturbance severity, *Ecology*, 96, 2478-2487, doi:10.1890/14-1810.1.
- Wang, H.: J.W. J. Riley, and W. D. Collins (2015), Statistical uncertainty of eddy covariance C02 fluxes inferred using a residual bootstrap approach, Agric. Far. Metearol., 206, 163-171.